J|A|C|S
ARTICLES

Crystal Engineering of Pharmaceutical Co-crystals: Application of Methyl Paraben as Molecular Hook

Mujeeb Khan, Volker Enkelmann, and Gunther Brunklaus*

Max-Planck-Institut für Polymerforschung, Postfach 31 48, D-55021 Mainz, Germany

Received January 7, 2010; E-mail: brunklaus@mpip-mainz.mpg.de

Abstract: Applicability of the O−H···N heterosynthon for synthesis of a pharmaceutical co-crystal comprised of a commonly used tablet excipient methyl paraben and quinidine, an anti-malarial constituent of *Cinchona* tree bark, has been successfully demonstrated. Insights into local conformation and hydrogen-bonding were derived from advanced multinuclear solid-state NMR techniques, where interpretation of the obtained NMR data was supported by DFT quantum-chemical computations. Furthermore, an approach for selective separation of quinidine from its stereoisomer quinine based on the *molecular specificity* of methyl paraben is presented. It was found that methyl paraben picked its target via hydrogen-bond-mediated molecular recognition, thereby acting as "*molecular hook*".

1. Introduction

Drug molecules with limited aqueous solubility are rather challenging in pharmaceutical development and may pose the risk of insufficient or inconsistent exposure and thus poor efficacy in patients upon oral administration.[1] Though numerous strategies exist for enhancing the bioavailability of drugs, these approaches often depend on the physicochemical nature of the considered molecules, which hampers widespread application.[2] Most pharmaceutical active ingredients (APIs) are crystalline solids at ambient temperature and conveniently delivered in solid oral dosage forms (i.e., tablets). Notably, fast-dissolving tablet (FDT) formulation may increase the oral availability of medicinal substances, but administration of FDTs is different from that of conventional tablets and requires properly chosen excipients (pharmaceutically inactive compounds such as coatings, filler, diluents, stabilizer, or preservatives).[3] Ideally, the drug's properties should not significantly affect the tablet characteristics, but often the tablet performance is vitiated.[4] Indeed, it is well known that fundamental properties of (crystalline) materials originate from molecular arrangements within the solid, and altering the placement and/or interactions between these molecules typically has a direct impact on the properties of the particular solid.[5] *Crystal engineering* comprises rational design and tailored fabrication of (functional) crystal structures[6] and hence offers manifold prospects to selectively enhance the physicochemical properties of drugs on the basis of in-depth knowledge of crystallization processes and molecular properties of APIs.[7−9] Notably, in addition to co-processing,[10] the concept of *co-crystallization* constitutes a selective route to the concerted design of pharmaceutical compounds with desired pharmacokinetic and physical properties.[3,11−13] However, the term "co-crystal" is not easily defined but is most commonly used in order to describe a crystal containing two or more

(1) (a) Blagden, N.; De Metas, M.; Gavan, P. T.; York, P. *Adv. Drug Delivery Rev.* **2007**, *59*, 617–630. (b) Huang, L. F.; Tong, W. Q. *Adv. Drug Delivery Rev.* **2004**, *56*, 321–324.
(2) (a) Amin, K.; Dannenfelser, R. M.; Zielinski, J.; Wang, B. *J. Pharm. Sci.* **2004**, *93*, 2244–2249. (b) Torchillin, V. P. *Pharm. Res.* **2007**, *24*, 1–16. (c) Humberstone, A. J.; Charman, W. N. *Adv. Drug Delivery Rev.* **1997**, *25*, 103–128.
(3) Jeong, S. H.; Takaishi, Y.; Fu, Y.; Park, K. *J. Mater. Chem.* **2008**, *18*, 3527–3535.
(4) Fu, Y.; Yang, S.; Jeong, S. H.; Kimura, S.; Park, K. *Crit. Rev. Ther. Drug* **2004**, *21*, 433–475.
(5) (a) Schultheiss, N.; Newman, A. *Cryst. Growth Des.* **2009**, *9*, 2950–2967. (b) Datta, S.; Grant, D. J. W. *Nat. Rev. Drug Discovery* **2004**, *3*, 42–57. (c) Chow, K.; Tong, H. H. Y.; Lum, S.; Chow, A. H. L. *J. Pharm. Sci.* **2008**, *97*, 2855–2877.
(6) (a) Khan, M.; Enkelmann, V.; Brunklaus, G. *J. Org. Chem.* **2009**, *74*, 2261–2270. (b) Khan, M.; Enkelmann, V.; Brunklaus, G. *CrystEngComm* **2009**, *11*, 1001–1005.
(7) (a) Desiraju, G. R. *Angew. Chem., Int. Ed.* **2007**, *46*, 8342–8356. (b) Desiraju, G. R. *Angew. Chem., Int. Ed. Engl.* **1995**, *34*, 2311–2327. (c) Desiraju, G. R. *Nat. Mater.* **2002**, *1*, 77–79. (d) Desiraju, G. R. *Nature (London)* **2001**, *412*, 397–400. (e) Desiraju, G. R. *Chem. Commun.* **1997**, *16*, 1474–1482. (f) Lehn, J. M. *Angew. Chem., Int. Ed. Engl.* **1990**, *29*, 1304–1319.
(8) (a) Childs, S. L.; Chyall, L. J.; Dunlap, J. T.; Smolenskaya, V. N.; Stahly, B. C.; Stahly, G. P. *J. Am. Chem. Soc.* **2004**, *126*, 13335–13342. (b) Remenar, J. F.; Morissette, S. L.; Peterson, M. L.; Moulton, B.; MacPhee, J. M.; Guzman, H. R.; Almarsson, O. *J. Am. Chem. Soc.* **2003**, *125*, 8456–8457. (c) Reddy, L. S.; Jagadeesh, N. B.; Nangia, A. *Chem. Commun.* **2006**, 1369–1371.
(9) (a) Fleischman, S. G.; Srinivasan, S. K.; McMahon, J. A.; Moulton, B.; Rosa, D.; Walsh, B.; Rodrguez-Hornedo, N.; Zaworotko, M. J. *Cryst. Growth Des.* **2003**, *3*, 909–919. (b) Walsh, R. D. B.; Bradner, M. W.; Fleischman, S.; Morales, L. A.; Moulton, B.; Rodriguez-Hornedo, N.; Zaworotko, M. J. *Chem. Commun.* **2003**, 186–187. (c) Almarsson, O.; Zaworotko, M. J. *Chem. Commun.* **2004**, 1889–1896. (d) McMahon, J. A.; Bis, J. A.; Vishweshwar, P.; Shattock, T. R.; McLaughlin, O. L.; Zaworotko, M. J. *Z. Kristallogr.* **2005**, *220*, 340–350.
(10) Gohel, M. C.; Jogani, P. D. *J. Pharm. Pharm. Sci.* **2005**, *8*, 76–93.
(11) (a) Childs, S. L.; Zaworotko, M. J. *Cryst. Growth Des.* **2009**, *9*, 4208–4211. (b) Shan, N.; Zaworotko, M. J. *Drug Discovery Today* **2008**, *13*, 440–446. (c) Weyna, D. R.; Shattock, T.; Vishweshwar, P.; Zaworotko, M. J. *Cryst. Growth Des.* **2009**, *9*, 1106–1123. (d) Bis, J. A.; Vishweshwar, P.; Weyna, D.; Zaworotko, M. J. *Mol. Pharmacol.* **2007**, *4*, 401–416.
(12) (a) Veber, D. F.; Stephen, R. J.; Cheng, H. Y.; Smith, B. R.; Ward, K. W.; Kopple, K. D. *J. Med. Chem.* **2002**, *45*, 2615–2623. (b) Stanton, M. K.; Tufekcic, S.; Morgan, C.; Bak, A. *Cryst. Growth Des.* **2009**, *9*, 1344–1352. (c) Jones, W.; Motherwell, W. D. S.; Trask, A. V. *MRS Bull.* **2006**, *31*, 875–879. (d) Good, D. J.; Rodriguez-Hornedo, N. *Cryst. Growth Des.* **2009**, *5*, 2252–2264.

Scheme 1. Hydrogen-Bond-Mediated *Molecular Recognition* of O−H···N Heterosynthon between Nitrogen-Bearing APIs and Parabens

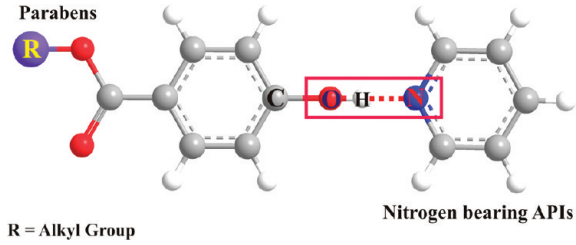

components that form a uniform phase, i.e., molecular complexes, solvates, clathrates, or inclusion compounds.[14] A more refined definition describes a co-crystal as a multi-component crystal that is formed between two compounds that are *solids* under ambient conditions, where at least one co-crystal former is molecular.[5a,15] Co-crystals often contain self-assembly units based on *supramolecular synthons* that are derived from motifs that are commonly found in crystal structures. In the case of pharmaceutical co-crystals, at least one of the components must be an API, while the additional co-crystal former(s) should be pharmaceutically acceptable, such as frequently used food additives and excipients.[5a,16,17] Though co-crystallization of APIs with multi-functional groups and ample conformational flexibility can be rather difficult, the use of even less crystalline or rather amorphous materials may yield improved properties (i.e., bioavailability).[18]

In the present work, we explore the applicability of the well-established, robust, and competetive O−H···N heterosynthon[19] for a reliable synthesis of pharmaceutical *multi-component co-crystals* using crystal engineering principles (cf. Scheme 1). Since both APIs and excipients comprise a vast variety of compounds, we selected the widely used preservative and food additive methyl paraben[20] (a simple ester of *p*-hydroxybenzoic acid) as molecular co-crystal former providing hydroxyl (OH) functional groups. On the other hand, we considered APIs that possess an accessible nitrogen, preferably embedded in an aromatic moiety (i.e., a pyridine-, quinolinide-, or acridine-type ring), such as quinidine. Quinidine is one of the anti-malarial constituents of *Cinchona* tree bark and is used as an anti-arrythmatic agent with anti-muscarinic and α-adrenoceptor blocking properties[21] or for treatment of neurological disorders.[22] In its pure form, however, quinidine is almost insoluble in

Scheme 2. Chemical Structures of the Two Alkaloid Stereoisomers Quinidine (11*S*,12*R*) and Quinine (11*R*,12*S*) as Well as the Common Excipient Methyl Paraben

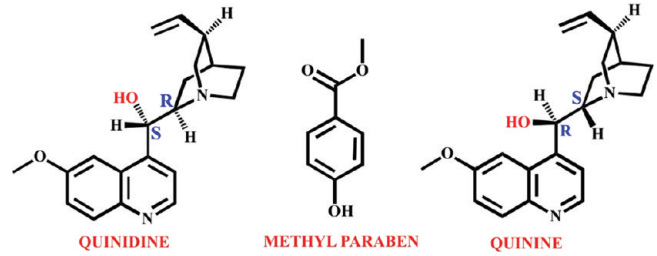

water,[23] rendering it an ideal candidate for co-crystallization. Successful formation of the binary co-crystal **1** was achieved from an equimolar mixture of quinidine and methyl paraben in ethanol. In addition, we have found that methyl paraben can be applied to *selectively* isolate quinidine from a mixture with quinine [an abundant stereoisomer of quinidine (cf. Scheme 2) present in *Cinchona* tree bark] by exploiting the molecular specificity (an important phenomenon in biological molecules)[24] of the O−H···N heterosynthon.

Apart from X-ray analysis, we utilized modern high-resolution solid-state NMR (i.e., at high magnetic fields and very fast magic-angle spinning), which in recent years has been shown to be a versatile and powerful tool for the characterization of (powdered) materials,[25] including pharmaceutical co-crystals and complexes.[26,27] Notably, NMR not only allows for non-invasive, element-specific observation of different nuclei, thereby providing outstanding selectivity for local environments[28] (even in rather ill-defined compounds), but also facilitates identification of chemically distinct sites based on NMR chemical shifts.[29] In particular, protons involved in hydrogen-bonded structures exhibit well-resolved ^{1}H chemical shifts, mainly between 8 and 20 ppm,[30] affording an estimation of hydrogen-bonding strengths.[31] Additional structural insights may be obtained from double-quantum ^{1}H MAS NMR,[32] where homonuclear ^{1}H−^{1}H

(13) (a) Morissette, S. L.; Almarsson, O.; Peterson, M. L.; Remenar, J. F.; Read, M. J.; Lemmo, A. V.; Ellis, S.; Cima, M. J.; Gardner, C. R. *Adv. Drug Delivery Rev.* **2004**, *56*, 275–300. (b) Trask, A. V. *Mol. Pharmaceutics* **2007**, *4*, 301–309.
(14) (a) Desiraju, G. R. *CrystEngComm* **2003**, *5*, 466–467. (b) Dunitz, J. D. *CrystEngComm* **2003**, *5*, 506–507.
(15) (a) Zuckerman-Schpector, J.; Tiekink, E. R. T. *Z. Kristalogr.* **2008**, *223*, 233–234. (b) Aakeroy, C. B.; Fasulo, M. E.; Desper, J. *Mol. Pharmaceutics* **2007**, *4*, 317–322. (c) Childs, S. L.; Stahly, G. P.; Park, A. *Mol. Pharmaceutics* **2007**, *4*, 323–338.
(16) (a) Vogt, M.; Kunath, K.; Dressman, J. B. *Eur. J. Pharm. Biopharm.* **2008**, *68*, 330–337. (b) Shakhtshneider, T. P.; Vasiltchenko, M. A.; Politov, A. A.; Boldyrev, V. V. *Int. J. Pharm.* **1996**, *130*, 25–32.
(17) (a) *Handbook of Pharmaceutical Salts: Properties, Selection and Use*; Sthal, P. H., Wermuth, C. G., Eds.; Verlag Helvetica Chimica Acta: Zürich, 2002. (b) GRAS Notices: http://www.cfsan.fda.gov/~rdb/opa-gras.html. (c) Food Additive status list: http://www.cfsan.fda.gov/~dms/opa-appa.html.
(18) Chow, K.; Tong, H. H. Y.; Lum, S.; Chow, A. H. L. *J. Pharm. Sci.* **2008**, *97*, 2855–2877.
(19) Khan, M.; Enkelmann, V.; Brunklaus, G. *Cryst. Growth Design* **2009**, *9*, 2354–2362.
(20) Soni, M. G.; Carabin, I. G.; Burdoc, G. A. *Food Chem. Toxicol.* **2005**, *43*, 985–1015.
(21) (a) Wahbi, A. M.; Moneed, M. S.; Hewala, I. I.; Bahnasy, M. F. *Chem. Pharm. Bull.* **2008**, *56*, 787–79. (b) Kashino, S.; Haisa, M. *Acta Crystallogr.* **1983**, *C39*, 310–312. (c) Pniewska, B.; Suszko-Purzycka, A. *Acta Crystallogr.* **1989**, *C45*, 638–642.
(22) Smith, R. A. *Exp. Opin. Pharmacother.* **2006**, *7*, 2581–2591.
(23) (a) Dijkstra, G. D. H.; Kellog, R. M.; Wynberg, H.; Svendsen, J. S.; Marko, I.; Sharpless, K. B. *J. Am. Chem. Soc.* **1989**, *111*, 8069–8076. (b) Silva, T. H. A.; Oliveira, A. B.; De Almeida, W. B. *Bioorg. Med. Chem.* **1997**, *5*, 353–361.
(24) (a) Mortison, J. D.; Kittendorf, J. D.; Sherman, D. H. *J. Am. Chem. Soc.* **2009**, *131*, 15784–15793. (b) Doyon, J. B.; Synder, T. M.; Liu, D. R. *J. Am. Chem. Soc.* **2003**, *125*, 12372–12373.
(25) (a) Reichert, D. *Annu. Rep. NMR Spectrosc.* **2005**, *55*, 159–203. (b) Ashbrook, S. E.; Smith, M. E. *Chem. Soc. Rev.* **2006**, *35*, 718–735. (c) Brown, S. P. *Prog. Nucl. Magn. Reson.* **2007**, *50*, 199–251.
(26) (a) Vogt, F. G.; Clawson, J. S.; Strohmeier, M.; Edwards, A. J.; Pham, T. N.; Watson, S. A. *Cryst. Growth Des.* **2009**, *9*, 921–937. (b) Vogt, F. G.; Vena, J. A.; Chavda, M.; Clawson, J. S.; Strohmeier, M.; Barnett, M. E. *J. Mol. Struct.* **2009**, *932*, 16–30.
(27) (a) Li, Z. J.; Abramov, Y.; Bordner, J.; Leonard, J.; Medek, A.; Trask, A. V. *J. Am. Chem. Soc.* **2006**, *128*, 8199–8210. (b) Terakita, A.; Matsunaga, H.; Ueda, T.; Eguchi, T.; Echigoya, M.; Umemoto, K.; Godo, M. *Chem. Pharm. Bull.* **2004**, *52*, 546–551.
(28) Orendt, A. M.; Facelli, J. C. *Annu. Rep. NMR Spectrosc.* **2007**, *62*, 115–178.
(29) (a) Harris, R. K. *Solid State Sci.* **2004**, *6*, 1025–1037. (b) Senker, J.; Seyfarth, L.; Voll, J. *Solid State Sci.* **2004**, *6*, 1039–1052.
(30) Chierotti, M. R.; Gobetto, R. *Chem. Commun.* **2008**, 1621–1634.
(31) Limbach, H. H. In *Hydrogen Transfer Reactions*; Hynes, J. T., Klinman, J. P., Limbach, H. H., Schowen, R. L., Eds.; Wiley-VCH: Weinheim, 2007.
(32) Brown, S. P.; Spiess, H. W. *Chem. Rev.* **2001**, *101*, 4125–4155.

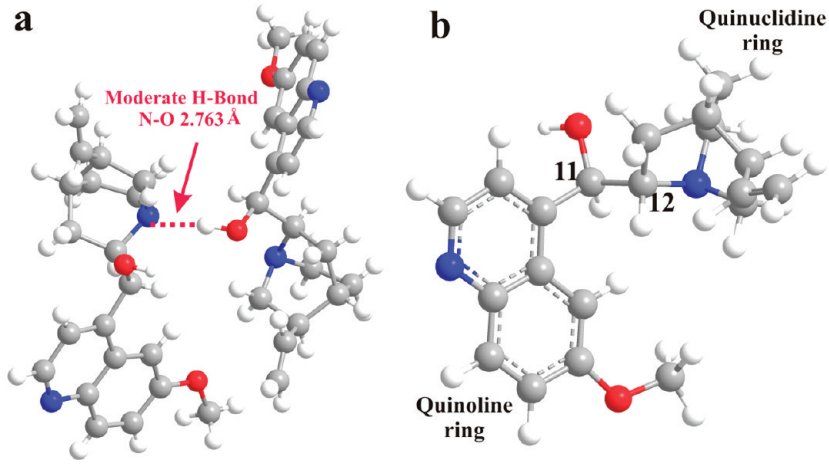

Figure 1. (a) Crystal structure projection of quinidine reflecting intermolecular hydrogen-bonding among two quinidine molecules. (b) 3D model of quinine (a crystal structure of quinine is not reported).[21c]

dipolar couplings correlate protons of different chemical entities, thereby providing precise information on both proton−proton distances on length scales of up to 3.5 Å[33] and proton positions in arrays of multiple hydrogen bonds.[34] In cases where exchangeable protons (such as OH or NH) are present, further spectral resolution may be obtained from ^{2}H MAS NMR. In most cases, ^{2}H MAS NMR chemical shifts agree well (within ±0.2 ppm)[35] with ^{1}H MAS NMR chemical shifts, thus allowing for an unambiguous assignment of proton positions. Packing effects such as hydrogen-bonding or π-stacking[36] are also reflected in ^{13}C or ^{15}N CPMAS NMR chemical shifts and can be analyzed via two-dimensional heteronuclear ^{1}H−^{13}C or ^{1}H−^{15}N correlation NMR experiments.[37] Moreover, the combination of solid-state NMR spectroscopy with density functional theory (DFT)[38] computations not only corroborates chemical shift assignments but also provides an approach to "NMR crystallography",[29,39] which allows for both polymorph screening,[40] e.g., in hydrochloride pharmaceuticals,[41] and even powder structure determination of small drug molecules.[42]

2. Results and Discussion

Quinidine (11*S*,12*R*) and quinine (11*R*,12*S*) are stereoisomers whose chemical structures differ only in the geometry of both

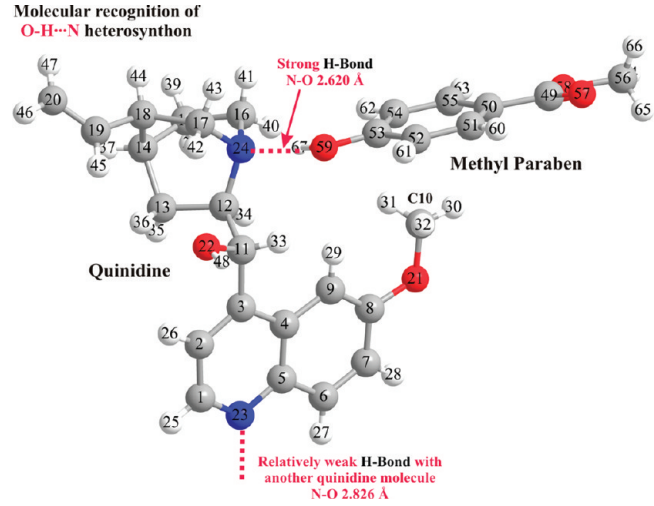

Figure 2. Binary, pharmaceutical co-crystal **1** obtained from quinidine and methyl paraben. The hydroxyl group of methyl paraben is strongly hydrogen-bonded to the quinuclidinic N-atom of quinidine.

the 11-hydroxyl group and the quinuclidine ring system, resulting in distinct orientations of the amine and hydroxyl groups relative to each other (Figure 1). From the viewpoint of crystal engineering based on the O−H···N heterosynthon, the nitrogen atoms of either the heteroaromatic quinoline or quinuclidine ring constitute possible targets for hydrogen-bond-mediated molecular recognition of hydroxyl groups offered by a suitable co-crystal former. In its pure form, however, quinidine crystallizes in a monoclinic space group [$P2_1$ (No. 4), $Z = 2$, $a = 11.883$ Å, $b = 7.037$ Å, $c = 11.256$ Å], with the unit cell comprised of two quinidine molecules that are stabilized by intermolecular hydrogen-bonding among the C11-hydroxyl group and the N-atom of the quinuclidine ring, while the N-atom of the quinoline ring remains "free" (cf. Figure 1).[21b]

Successful formation of the *pharmaceutical co-crystal* **1** (whose potentially beneficial properties are currently under investigation) was achieved from an equimolar mixture of quinidine and methyl paraben in ethanol (cf. Figure 2). It crystallizes in an orthorhombic space group [$P2_12_12_1$ (No. 19), $Z = 4$, $a = 9.962$ Å, $b = 11.497$ Å, $c = 22.710$ Å], where the

(33) Schulz-Dobrick, M.; Metzroth, T.; Spiess, H. W.; Gauss, J.; Schnell, I. *Chem. Phys. Chem.* **2005**, *6*, 315–327.
(34) (a) Schnell, I.; Langer, B.; Söntjens, S. H. M.; Sijbesma, R. P.; van Genderen, M. H. P.; Spiess, H. W. *Phys. Chem. Chem. Phys.* **2002**, *4*, 3750–3758. (b) Bolz, I.; Moon, C.; Enkelmann, V.; Brunklaus, G.; Spange, S. *J. Org. Chem.* **2008**, *73*, 4783–4793.
(35) Schulz-Dobrick, M.; Schnell, I. *Central Eur. J. Chem.* **2005**, *3*, 245–251.
(36) (a) Lazzeretti, P. *Prog. Nucl. Magn. Reson. Spectrosc.* **2000**, *36*, 1–88. (b) Gomes, J. A. N. F.; Mallion, R. B. *Chem. Rev.* **2001**, *101*, 1301–1315.
(37) Saalwächter, K.; Schnell, I. *Solid State Nucl. Magn. Reson.* **2002**, *22*, 154–187.
(38) (a) Geerlings, P.; De Proft, F.; Langenaeker, W. *Chem. Rev.* **2003**, *103*, 1793–1873. (b) Parr, R. G.; Yang, W. *Density Functional Theory of Atoms and Molecules*; Oxford University Press: Oxford, 1989.
(39) (a) Elena, B.; Pintacuda, G.; Mifsud, N.; Emsley, L. *J. Am. Chem. Soc.* **2006**, *128*, 9555–9560. (b) Pickard, C. J.; Salager, E.; Pintacuda, G.; Elena, B.; Emsley, L. *J. Am. Chem. Soc.* **2007**, *129*, 8932–8933. (c) Taulelle, F. *Solid State Sci.* **2004**, *6*, 1053–1057. (d) Seyfarth, L.; Seyfarth, J.; Lotsch, B. V.; Schnick, W.; Senker, J. *Phys. Chem. Chem. Phys.* **2007**, *12*, 2227–2237.
(40) (a) Harris, R. K. *J. Pharm. Pharmacol.* **2007**, *59*, 225–239. (b) Harris, R. K. *Analyst* **2006**, *131*, 351–373.
(41) Hamaed, H.; Pawlowski, J. M.; Cooper, B. F. T.; Fu, R.; Eichhorn, S. H.; Schurko, R. W. *J. Am. Chem. Soc.* **2008**, *130*, 11056–11065.
(42) Salanger, E.; Stein, R. S.; Pickard, C. J.; Elena, B.; Emsley, L. *Phys. Chem. Chem. Phys.* **2009**, *11*, 2610–2621.

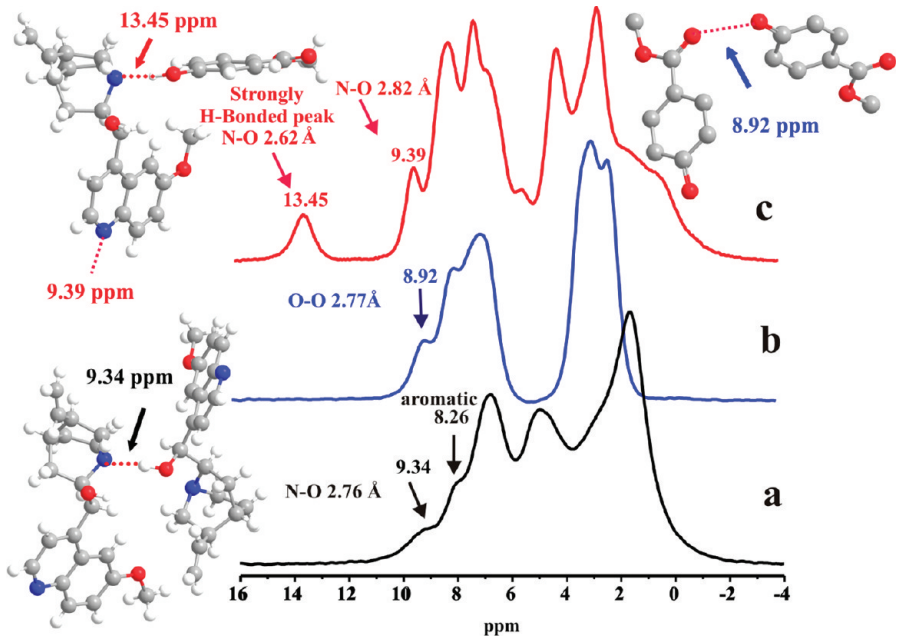

Figure 3. ^{1}H MAS NMR spectra of (a) quinidine, (b) methyl paraben, and (c) co-crystal **1**, acquired at 850.1 MHz using a commercially available Bruker 1.3 mm double-resonance MAS probe at a spinning frequency of 50 kHz, typical $\pi/2$ pulse lengths of 2 μs, and recycle delays of 5−10 s, co-adding 32 transients.

asymmetric unit is comprised of a hydrogen-bonded 1:1 complex of quinidine and methyl paraben. The unit cell consists of four quinidine and four methyl paraben molecules, respectively, resulting in a significantly larger *c*-axis. In **1**, the quinuclidinic N-atom is hydrogen-bonded to the OH-group of methyl paraben, while the N-atom of the quinoline ring connects two quinidine molecules (cf. Figure 2). In this way, the molecular arrangement in **1** is clearly governed by a two-fold "application" of the O−H···N heterosynthon, while the overall conformation of quinidine in **1** resembles the conformation of pure quinidine, except for a rotation of the quinoline ring's methoxy group changing from an *anti*-conformation with respect to the terminal carbon (C9) of the quinoline ring to a *syn*-conformation in **1**. In contrast, a co-crystal of methyl paraben and quinine could *not* be obtained, probably owing to the conformational differences.

Though selective hydrogen-bonding is the preferred interaction in many crystal engineering studies[43] and is known to contribute to the physical properties and reactivity of molecular complexes and supramolecular aggregates, its characterization by X-ray analysis is difficult, even with sophisticated powder X-ray diffraction.[44] The hydrogen bonds considered here, however, fall within the range of "*classical*" strong hydrogen bonds, where the distances of the heavy atoms are less than the sum of their van der Waals radii (N···O 3.22 Å, O···O 3.04 Å).[45] Nevertheless, on the basis of the separation of heavy atoms involved, the intermolecular hydrogen bond between two quinidine molecules in **1** can be regarded as weaker than the hydrogen bond between quinidine and methyl paraben (cf. Figure 2). In case of dynamic hydrogen-bonding, i.e., exchange of the proton among two heavy atoms with a given distance,[46] the "effective strength" of the hydrogen bond can be conveniently identified by ^{1}H MAS NMR: typical evidence of strong hydrogen-bonding is high-frequency-shifted ^{1}H resonances, i.e., at 16−22 ppm for hydrogen bonds to nitrogen or oxygen.[47]

Solid-State NMR Characterization of the Co-crystal. The ^{1}H fast MAS NMR spectrum of **1** (cf. Figure 3) exhibits two resonances at 9.39 and 13.45 ppm that are indicative of moderate and rather strong hydrogen-bonding, respectively. The latter signal is neither present in the ^{1}H MAS NMR spectrum of quinidine nor that of methyl paraben; therefore, it reveals formation of a new hydrogen bond. Indeed, this is consistent with the refined heavy-atom separations in the corresponding crystal structures: in **1**, the quinuclidinic N-atom is strongly hydrogen-bonded to the OH group of methyl paraben (H67) (d(N−O) = 2.620 Å) replacing the moderate intermolecular hydrogen-bond (d(N−O) = 2.763 Å) between two quinidine molecules in its pure form, whereas the N-atom of the quinoline ring is now involved in a fairly weak hydrogen bond (d(N−O) = 2.826 Å) connecting *two* quinidine molecules via the hydroxyl proton of quinidine (H48). Since hydroxyl protons can be exchanged with deuterons, deuterated samples of both **1** and pure quinidine were prepared and characterized by ^{2}H MAS NMR (cf. Figure 4). In the case of quinidine, a single peak at 8.95 ppm is observed, while two signals at 13.35 and 8.94 ppm are found in the case of the co-crystal supporting the ^{1}H MAS NMR peak assignment (H67, 13.45 ppm; H48, 9.39 ppm). Note the slightly weaker hydrogen bond involving "D48" (the corresponding ^{13}C CPMAS spectrum of **1**-d_2 is identical to that of **1**). Such selective measurements are particularly useful for an unambiguous characterization of powdered pharmaceutical co-compounds where either the crystal structure is *not* known or rather crowded spectra with severe peak overlaps are obtained.

In principle, when the experimentally observed ^{1}H MAS NMR line shapes are broadened solely by strong homonuclear

(43) (a) Aakeroy, C. B.; Beatty, A. M. *Aust. J. Chem.* **2001**, *54*, 409–421. (b) Desiraju, G. R. *Acc. Chem. Res.* **2002**, *35*, 565–573.
(44) Harris, K. D. M.; Cheung, E. Y. *Chem. Soc. Rev.* **2004**, *33*, 526–538.
(45) Frey, P. A. *Magn. Reson. Chem.* **2001**, *39*, S190–S198.
(46) Khan, M.; Brunklaus, G.; Enkelmann, V.; Spiess, H. W. *J. Am. Chem. Soc.* **2008**, *130*, 1741–1748.
(47) Gobetto, R.; Nervi, C.; Valfrè, E.; Chierotti, M. R.; Braga, D.; Maini, L.; Grepioni, F.; Harris, R. K.; Ghi, P. Y. *Chem. Mater.* **2005**, *17*, 1457–1466.

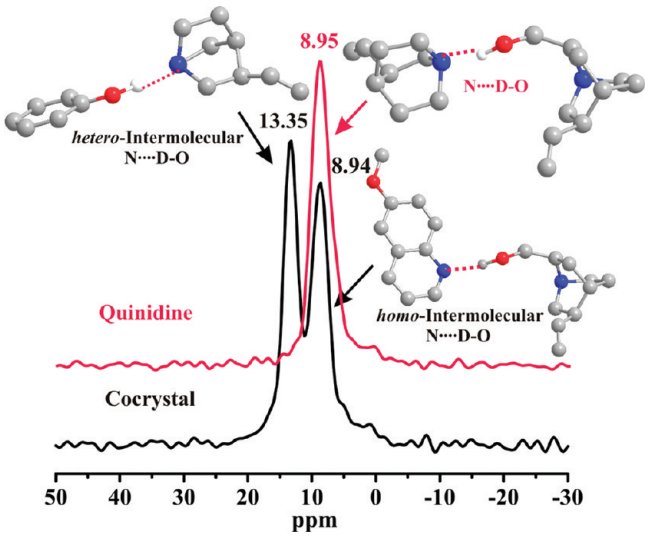

Figure 4. ^{2}H MAS NMR spectra of **1**-d_2 (co-crystal) and quinidine-d_1, acquired at 46.7 MHz using a commercially available Bruker 2.5 mm triple-resonance MAS probe at a spinning frequency of 20 kHz, typical $\pi/2$ pulse lengths of 2.5 μs, and recycle delays of 5 s, co-adding 8196 transients. Spectra were referenced with respect to solid dimethylsulfone (DMS, 3.4 ppm).

dipolar couplings among abundant protons, high-resolution solid-state ^{1}H MAS NMR spectra can be obtained employing so-called homonuclear dipolar decoupling sequences such as windowed phase-modulated Lee−Goldburg (wPMLG)[48] or windowed DUMBO-1,[49] which also constitute the key part of double-quantum spectra (DQ-CRAMPS).[50] This approach, however, requires a high degree of local order, thus limiting its applications when dealing with polycrystalline or structurally less-defined powdered samples that may result from early co-crystallization attempts. In such cases, the application of fast MAS is more convenient.

^{1}H−^{1}H double-quantum (DQ) MAS NMR is in general a highly useful and selective approach to identify close contacts or spatial proximities of structural moieties and can be used to reveal changes of (local) hydrogen-bonding environments, i.e., upon successful formation of a pharmaceutical co-compound. In such a two-dimensional experiment, DQ coherences due to pairs of dipolar coupled protons are correlated with single-quantum coherences, resulting in characteristic correlation peaks. Double-quantum coherences between *like* spins appear as a single correlation peak on the diagonal, while a pair of cross-peaks that are symmetrically arranged on either side of the diagonal reflect couplings among *unlike* spins. In addition, at short dipolar recoupling times (i.e., 20 − 40 μs), observable DQ signal intensities are proportional to D_{ij}^2 or r_{ij}^{-6} (D_{ij} is the homonuclear dipolar coupling constant; r_{ij} is the internuclear distance), respectively, so that strong signal intensities in the corresponding DQ MAS NMR spectrum indicate protons in rather close spatial proximity. In contrast, rather weak DQ signals reflect either long-distance contacts or the presence of fast local molecular dynamics (with respect to the time scale of the experiment).[51] The corresponding ^{1}H−^{1}H DQ MAS NMR spectrum of **1** is displayed in Figure 5. Notably, the experiment was performed at a high spinning frequency of 50 kHz in order to maximize the achievable spectral resolution in the indirect dimension (F1) of the experiment. This is particularly necessary at the magnetic field of 20 T (^{1}H, 850.1 MHz) if the spectral window (that covers the peaks of interest in the 1D ^{1}H MAS NMR spectrum) exceeds 17.5 ppm (ca. 14.9 kHz). In such a case, the routinely applied MAS frequency of 30 kHz may lead to folding of DQ signals, which evolve at the sum of the chemical shifts of the dipolar coupled spins.

According to the crystal structure of **1**, the hydroxyl proton (H67, 13.4 ppm) of methyl paraben mainly has three close proton contacts up to 3.5 Å: aliphatic protons of the quinuclidine ring [H34, H40, H41, H42, H43 (cf. Figure 2)], proton (H33) attached to the carbon (C11) that connects the quinoline and quinuclidine rings, and aromatic protons of methyl paraben (H62, H61). While the DQ cross peak at 16.1 ppm (13.4 + 2.7 ppm) originates from contacts of H67 (hydroxyl proton of methyl paraben) with aliphatic protons, the slightly stronger DQ cross-peak at 19.8 ppm (13.4 + 6.4 ppm) reflects its contact with aromatic protons of methyl paraben (H61, H62), hence proving the hydrogen-bonded complex of quinidine and methyl paraben that comprises the asymmetric unit of **1**. An additional strong DQ cross-peak at 17.6 ppm (9.3 + 8.3 ppm) reflects the close spatial proximity of the quinidine hydroxyl proton (H48, 9.3 ppm) to aromatic protons of the quinoline ring (H25, H27, 8.3 ppm) of a neighboring molecule and thus provides insights into the molecular packing of **1**. All other DQ peaks represent rather trivial DQ contacts among aliphatic and/or aromatic protons and are in agreement with the crystal structure. Notably, the lack of a DQ correlation peak among H67 and methoxy protons of methyl paraben [H64, H65, H66 (cf. Figure 2)] indicates a different hydrogen-bonding environment of methyl paraben in **1** compared to that of pure methyl paraben, where the hydroxyl proton is hydrogen-bonded to carbonyl oxygen O57. In favorable cases, particularly in the case of dipolar coupled clusters (i.e., triple or quadruple hydrogen-bonded moieties), selected internuclear proton−proton distances (derived from ^{1}H−^{1}H dipolar couplings) may be conveniently elucidated if the so-called DQ spinning sideband pattern can be generated.[52] While this approach has been successfully used to investigate, e.g., the helical arrangement of benzoxazine oligomers[53] or columnar packing of selectively deuterated hexabenzocoronene,[54] its application to more complex or rather amorphous systems is often hampered by distribution effects[55] or insufficient spectral resolution.

Since nitrogen-based heterocycles are rather commonly present in pharmaceutical compounds, further insights into the hydrogen-bonding network and local structural environments may be obtained from ^{15}N CPMAS NMR. The ^{15}N chemical shift is quite sensitive to packing effects and often provides superior resolution, particularly in cases where the nitrogen atoms are partially protonated. Due to rather low natural

(48) (a) Leskes, M.; Madhu, P. K.; Vega, S. *J. Chem. Phys.* **2008**, *128*, 052309/1–052309/11. (b) Leskes, M.; Madhu, P. K.; Vega, S. *J. Chem. Phys.* **2006**, *125*, 124506/1–124506/18.
(49) Lesage, A.; Sakellariou, D.; Hediger, S.; Elena, B.; Charmont, P.; Steuernagel, S.; Emsley, L. *J. Magn. Reson.* **2003**, *163*, 105–113.
(50) Brown, S. P.; Lesage, A.; Elena, B.; Emsley, L. *J. Am. Chem. Soc.* **2004**, *126*, 13230–13231.
(51) Bradley, J. P.; Tripon, C.; Filip, C.; Brown, S. P. *Phys. Chem. Chem. Phys.* **2009**, *11*, 6941–6952.
(52) Friedrich, U.; Schnell, I.; Brown, S. P.; Lupulescu, A.; Demco, D. E.; Spiess, H. W. *Mol. Phys.* **1998**, *95*, 1209–1227.
(53) Goward, G. R.; Sebastiani, D.; Schnell, I.; Spiess, H. W.; Kim, H. D.; Ishida, H. *J. Am. Chem. Soc.* **2003**, *125*, 5792–5800.
(54) Brown, S. P.; Schnell, I.; Brand, J. D.; Müllen, K.; Spiess, H. W. *J. Am. Chem. Soc.* **1999**, *121*, 6712–6718.
(55) Holland, G. P.; Cherry, B. R.; Alam, T. M. *J. Magn. Reson.* **2004**, *167*, 161–167.

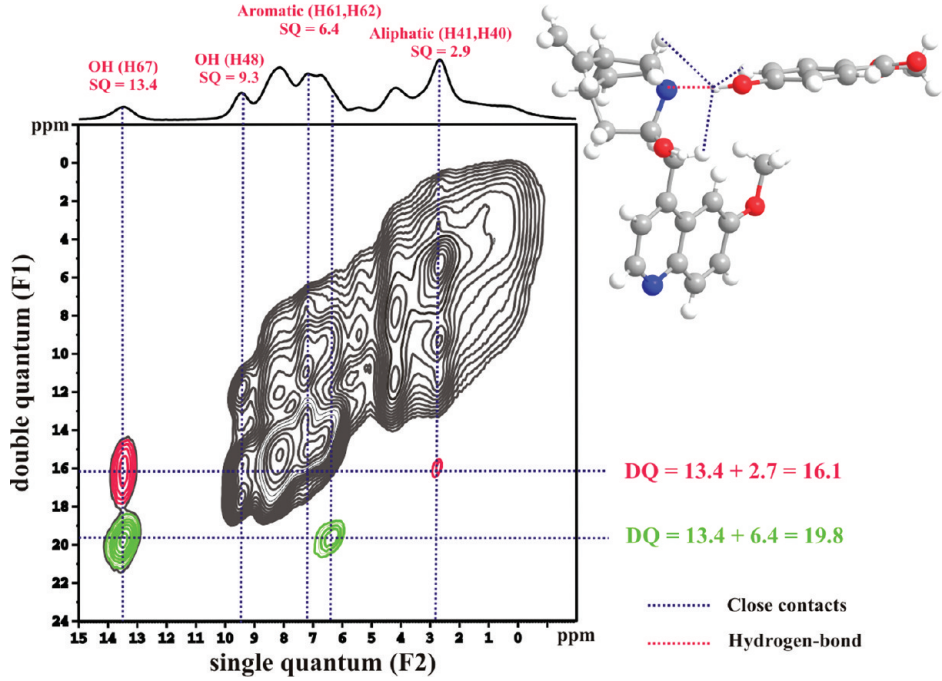

Figure 5. $^{1}H-^{1}H$ DQ MAS NMR spectrum of the co-crystal **1** at 850.1 MHz and 50 kHz MAS, acquired under the following experimental conditions: $\tau_{(exc)} = 20\ \mu s$, 64 t_1 increments at steps of 20 μs, relaxation delay 60 s, 16 transients per increment. Sixteen positive contour levels between 4% and 98% of the maximum peak intensity were plotted. The F2 projection is shown on the top; the most important DQ cross-peaks are highlighted.

abundance of the NMR-active isotope (^{15}N, 0.36%), however, either large sample amounts or selective labeling is often required to reduce the otherwise long acquisition times.[56] In the case of **1**, two resonances at −91.7 and −346.4 ppm, respectively, were observed in the 1D ^{15}N CPMAS spectrum (cf. Figure 6), while the corresponding spectrum of pure quinidine displays signals at −73.6 and −344.0 ppm. Indeed, the peak assignment is not trivial. On a first glance, on the basis of the significant shortening of the N−O distance from 2.76 to 2.62 Å upon co-crystal formation, one might be tempted to assign the ^{15}N peak that shifts from −73.6 (pure quinidine) to −91.7 ppm to the N-atom of the quinuclidine ring (N24) of **1**. On the other hand, one has to take into account that the previously "free" N-atom of the quinoline ring in pure quinidine upon co-crystal formation is hydrogen-bonded to a neighboring quinidine molecule, which also represents a significant change of the local environment.

For a heterocyclic and fairly basic nitrogen, an upfield shift (i.e., larger negative ppm values) of about 20 up to 40 ppm has been reported in the case of rather strong hydrogen-bonding, while upfield shifts of even 80 ppm or greater may occur if a proton is transferred from a donor (such as a carboxylic acid) to an acceptor nitrogen.[27a] Since we similarly observe an upfield shift of about 18 ppm, we assign the ^{15}N peaks at −73.6 and −91.7 ppm, respectively, to the corresponding N-atom of the quinoline ring in both pure quinidine and the co-crystal. Consequently, the resonances at −344.0 and −346.4 ppm can be attributed to the N-atom of the quinuclidine ring, indicating only a marginal upfield shift of about 2.5 ppm upon co-crystallization. Notably, the absence of stronger upfield shifts

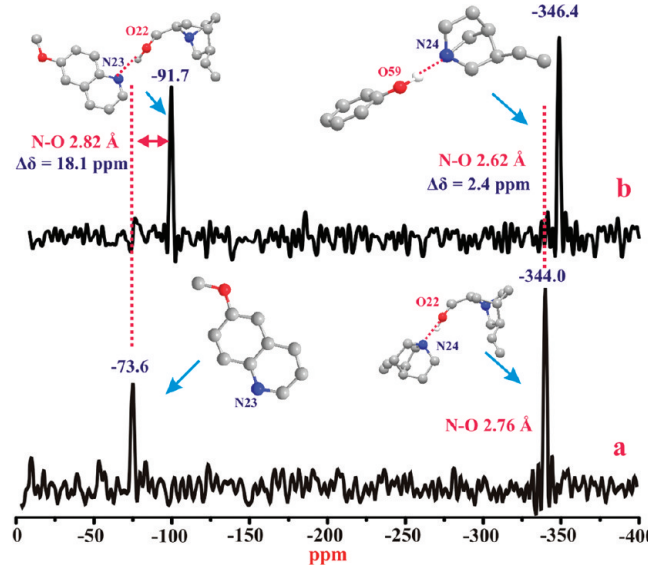

Figure 6. ^{15}N CPMAS NMR spectra of (a) pure quinidine and (b) co-crystal **1**, acquired at 125.77 MHz using a Bruker Avance-II 300 machine with a contact time of 2 ms, co-adding 4096 transients. The experiments were carried out using a Bruker 4 mm double-resonance MAS probe spinning at 12 kHz, typical $\pi/2$ pulse length of 4 μs, and a recycle delay of 40 s.

(i.e., ≥80 ppm) on going from pure quinidine to the co-crystal **1** clearly rules out a possible salt formation.

The ^{15}N peak assignment is supported by DFT chemical shift computations based on selected fragments of the crystal structures (i.e., the asymmetric unit of **1** and a quinidine dimer). The corresponding proton positions were optimized at the B3LYP/6-311+G** level of theory, while the heavy atoms were fixed at the crystallographic positions. While this approach is rather simplistic (i.e., ignoring possible influences of the periodic crystal packing), the computed ^{15}N chemical shifts are neverthe-

(56) (a) Foces-Foces, C.; Echevarria, A.; Jagerovic, N.; Alkorta, I.; Elguero, J.; Langer, U.; Klein, O.; Minguet-Bonvehi, M.; Limbach, H.-H. *J. Am. Chem. Soc.* **2001**, *123*, 7898–7906. (b) Lorente, P.; Shenderovich, I. G.; Golubev, N. S.; Denisov, G. S.; Buntkowsky, G.; Limbach, H.-H. *Magn. Reson. Chem.* **2001**, *39*, S18–S29.

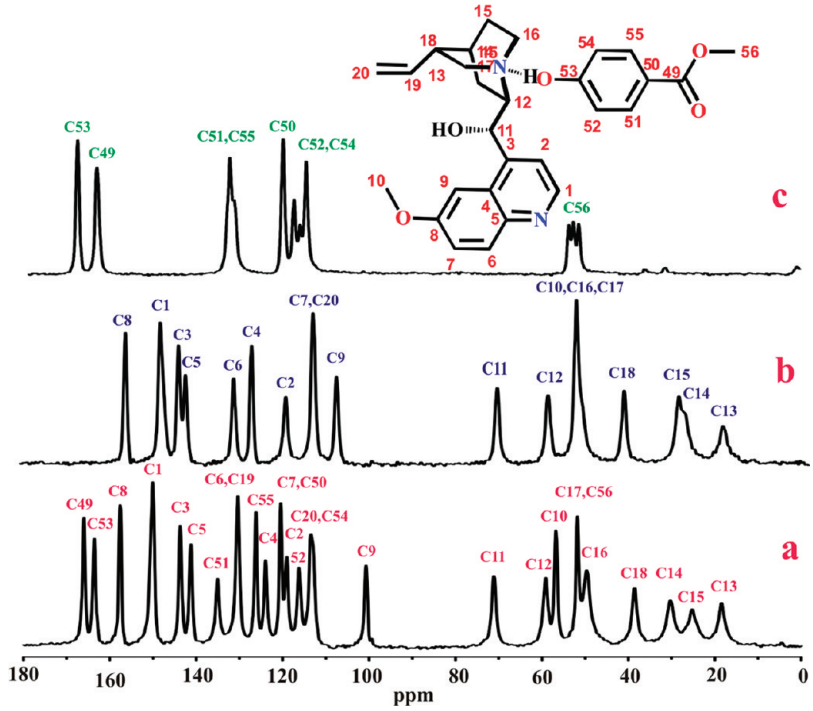

Figure 7. Solid-state ^{13}C CPMAS spectra of (a) co-crystal **1**, (b) quinidine, and (c) methyl paraben. All ^{13}C CPMAS spectra were collected at 125.77 MHz using a Bruker Avance-II 300 machine with a contact time of 2 ms, co-adding 8196 transients. The experiments were carried out using a standard 4 mm double-resonance MAS probe spinning at 12 kHz, typical $\pi/2$ pulse length of 4 μs, and a recycle delay of 5 s. All spectra were acquired at room temperature, while the given peak assignments are based on DFT computations.

less accurate enough to allow for an unambiguous peak assignment. In the case of the co-crystal **1**, the computed ^{15}N chemical shifts of the nitrogen atoms of both the quinoline (N23) and quinuclidine ring (N24) amount to −54.1 and −350.6 ppm, respectively. Similarly for quinidine, representative shifts of −60.1 and −351.3 ppm were obtained. A comparison of the computed and experimental shifts indicates that the experimentally observed trends are reasonably reproduced, particularly the explicit chemical shift of the quinuclidinic N-atom (within ±5 ppm) and marginal upfield shift upon co-crystallization. The rather large deviation of the predicted ^{15}N chemical shifts of the quinolinic N-atom, however, can be most likely attributed to the simplicity of the chosen fragments; nevertheless, the experimental ^{15}N chemical shift separation of more than 254 ppm renders the obtained ^{15}N shift values acceptable. Further confidence originates from the fact that the ^{1}H chemical shift of the hydroxyl proton H67 at an optimized position within the frozen N−O distance in the asymmetric unit of **1** is computed at 13.8 ppm, which is in good agreement (±0.4 ppm) with the experimental shift of 13.45 ppm.

In addition to ^{1}H and ^{15}N NMR spectra, ^{13}C CPMAS NMR spectra were recorded (cf. Figure 7) to monitor structural features and differences of the starting compounds and **1**, as the ^{13}C chemical shifts are sensitive to even small changes in the local environment (and hence can be considered as a "fingerprint"). This becomes particularly handy when less-ordered or even amorphous compounds are obtained, i.e., during a rapid screening of potential co-crystal formers with respect to a target compound. While solution ^{13}C NMR data (cf. Supporting Information) may provide initial peak assignments of molecular fragments, ^{13}C chemical shifts in the solid state are often influenced by different conformations and/or packing effects such as $\pi-\pi$-interactions. Therefore, we have assigned the ^{13}C chemical shifts on the basis of DFT computations using the recently introduced multi-standard (MSD) approach.[57] Though in the case of known crystal structures, more sophisticated and computationally demanding but highly accurate chemical shift computations employing periodic boundary conditions are feasible,[58] the MSD approach is sufficiently accurate and computationally rather cheap and thus allows for faster screening if only structural fragments of potential target co-compounds (e.g., identified from multi-dimensional NMR on powdered samples) are known. The corresponding ^{13}C CPMAS spectra of quinidine, methyl paraben, and the co-crystal **1** are shown in Figure 7. In the case of **1**, well-resolved peaks are found, which allows us to distinguish individual signals (i.e., due to quinidine or methyl paraben).

Most ^{13}C signals of quinidine within the co-crystal **1** displayed minor changes of 1−2 ppm owing to a slightly different molecular packing, while a few carbons revealed a drastic change. In particular, the signals of C7 (downfield shifted from 113.8 to 120.4 ppm) and C9 (upfield shifted from 107.8 to 100.6 ppm) of the quinoline ring have shifted about 7 ppm, reflecting the changed conformation of the methoxy group (C10) in **1**. In pure quinidine, carbon C10 of the methoxy group was in *anti*-conformation with respect to the aromatic carbon C9 and *syn*-conformation with respect to the carbon C7 (cf. Figure 1a). In the co-crystal, however, after bond rotation, it has adopted

(57) Sarotti, A. M.; Pellegrinet, S. C. *J. Org. Chem.* **2009**, *74*, 7254–7260.
(58) (a) Zurek, E.; Pickard, C. J.; Autschbach, J. *J. Am. Chem. Soc.* **2007**, *129*, 4430–4439. (b) Uldry, A. C.; Griffin, J. M.; Yates, J. R.; Perez-Torralba, M.; Maria, M. D. S.; Webber, A. L.; Beaumont, M. L. L.; Samoson, A.; Claramunt, R. M.; Pickard, C. J.; Brown, S. P. *J. Am. Chem. Soc.* **2008**, *130*, 945–954. (c) Harris, R. K.; Ghi, P. Y.; Hammond, R. B.; Ma, C. Y.; Roberts, K. J.; Yates, J. R.; Pickard, C. J. *Magn. Reson. Chem.* **2006**, *44*, 325–333. (d) Yates, J. R.; Dobbins, S. E.; Pickard, C. J.; Mauri, F.; Ghi, P. Y.; Harris, R. K. *Phys. Chem. Chem. Phys.* **2005**, *7*, 1402–1407. (e) Zheng, A.; Liu, S.-B.; Deng, F. *J. Comput. Chem.* **2009**, *30*, 222–235.

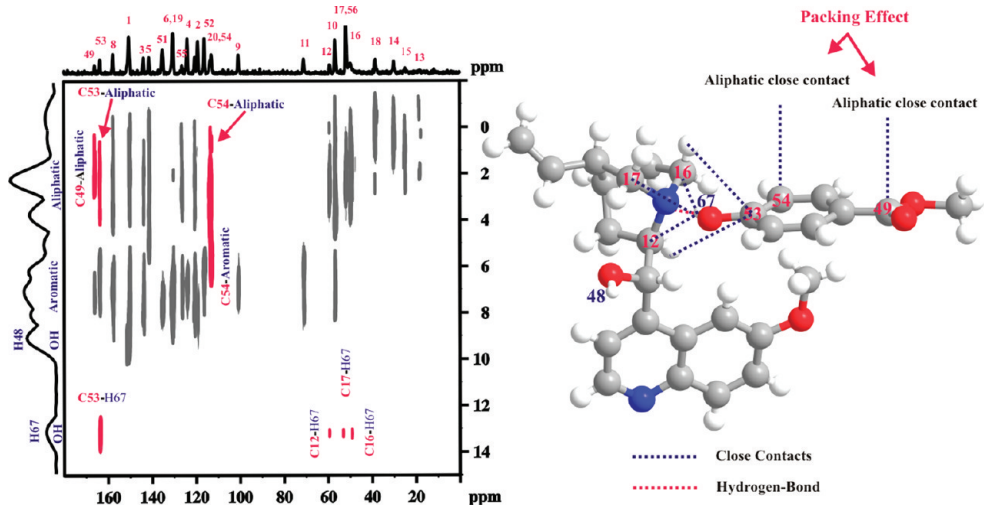

Figure 8. $^{1}H-^{13}C$ CP-HETCOR spectrum of **1** acquired on an 850.1 MHz Bruker Avance III spectrometer, using a commercially available Bruker 1.3 mm double-resonance MAS probe at a spinning frequency of 50 kHz. Typical $\pi/2$ pulse lengths of 2 μs for ^{1}H and 5 μs for ^{13}C with a contact time 2 ms were used. In addition, $\tau_{(exc)} = 20$ μs, 64 t_1 increments at steps of 20 μs, relaxation delay 5 s, and 720 transients per increment have been added. Sixteen positive contour levels between 4% and 98% of the maximum peak intensity were plotted. The F2 projection is shown on the top; the most important correlation peaks are highlighted.

opposite conformations (cf. Figure 2) to avoid steric hindrance (i.e., *syn*-conformation with respect to C9 and *anti*-conformation with respect to C7). In addition, the carbon signals of methyl paraben in **1** also experienced significant shifts compared to those of the pure form, where especially C49 (downfield shifted from 164.2 to 166.2 ppm) and C53 (upfield shifted from 168.7 to 163.6 ppm) reflect the different hydrogen-bonding environments. In pure methyl paraben, the hydroxyl group is hydrogen-bonded to the carbonyl oxygen (O57), while in the co-crystal **1**, it has formed a strong hydrogen bond to the quinuclidine nitrogen (N24) so that the carbonyl oxygen remains "free". It should be noted that the ^{13}C CPMAS spectrum of pristine methyl paraben (cf. Figure 7c), at a first glance, displays more signals than expected from the molecular structure [i.e., three different signals appear at ~51 ppm for the methoxy carbon (C56), while only one signal is expected], which can be attributed to the fact that the asymmetric unit consists of three paraben molecules.[59] Indeed, this has been frequently found for molecular crystals[60] and used for "NMR crystallography".[39]

The molecular packing (and identity) of the co-crystal **1** is further verified via a two-dimensional $^{1}H-^{13}C$ CP-HETCOR spectrum (cf. Figure 8). In such an experiment, correlation peaks are generated via dipolar coupling-driven magnetization transfer, where proper setting of the contact time allows us to distinguish both short-range and long-range contacts.[61] Indeed, this can be utilized to clearly identify interacting sites, particularly in potential pharmaceutical co-crystals where both the API and co-crystal former(s) may form hydrogen bonds among themselves. The $^{1}H-^{13}C$ CP-HETCOR spectrum of the co-crystal **1** (cf. Figure 8) shows a number of correlation peaks that evidence close spatial proximity of methyl paraben to quinidine: correlation between the aliphatic carbons of quinuclidine ring (C12, C16, C17) and the hydroxyl proton (H67) of methyl paraben as well as correlation between C53 (to which the hydroxyl group is attached) of methyl paraben and the aliphatic protons of the quinuclidine ring (H40, H41, etc.) that are present at distances of less than 3 Å. Furthermore, the correlation of the carbonyl carbon (C49) with aliphatic protons, as well as the correlation of the aromatic carbon (C54) of methyl paraben with aliphatic protons of the quinuclidine ring, originates from long-range (3−5 Å) packing effects which clearly indicate successful co-compound formation (even in the absence of a crystal structure).

Application of Methyl Paraben as Molecular Hook. The use of specific interactions to tailor desired properties or provide means of separation is a central challenge in chemistry. Selections based on *molecular specificity* (the processes of physically separating molecules with favorable properties from inactive molecules) offer much higher potential throughput than mere screens and typically do not require sophisticated equipment.[6a,24b,62] Hence, we have tested the molecular specificity of methyl paraben for its potential to *selectively isolate* quinidine from a mixture composed of quinidine and quinine. While separation of the stereoisomers (i.e., from blood samples after oral dosage or crude extract of *Cinchona* tree bark) is typically based on sophisticated protocols using high-performance liquid chromatography (HPLC),[63] one-pot separation based on co-crystallization could be beneficial. As mentioned above, quinidine yielded colorless prism-like co-crystals with methyl paraben upon slow evaporation in ethanol, while the use of quinine, however, under similar conditions resulted in a colorless, rather glassy substance that sticks to the walls and bottom of the beaker. The (apparent) lack of molecular recognition of quinine by methyl paraben could originate from the "*closed*" conformation of the quinine molecule (cf. Figure 1b), where both the quinoline and quinuclidine rings are closer to each other, forming an *arc*, probably owing to the flexibility of carbon (C11) connecting them. Due to this, the hydroxyl group (OH) of methyl paraben may not have an easy access to the nitrogen of the quinoclidine ring, unlike in the rather "*open*" conformation of quinidine, which renders the acceptor nitrogen

(59) (a) Vujovic, D.; Nassimbeni, L. R. *Cryst. Growth Des.* **2006**, *6*, 1595–1597. (b) Lin, X.; Chin, T. *J. Struct. Chem.* **1983**, *2*, 213–215.
(60) (a) Harris, R. K. *Analyst* **2006**, *131*, 351–373. (b) Masuda, K.; Tabata, S.; Kono, H.; Sakata, Y.; Hyyase, T.; Yonemochi, E.; Tarada, K. *Int. J. Pharm.* **2006**, *318*, 146–153.
(61) Brus, J.; Jegorov, A. *J. Phys. Chem. A* **2004**, *108*, 3955–3964.
(62) (a) Taylor, S. V.; Kast, P.; Hilvert, D. *Angew. Chem., Int. Ed.* **2001**, *40*, 3310–3335. (b) Lin, H.; Cornish, V. W. *Angew. Chem., Int. Ed.* **2002**, *41*, 4402–4425.
(63) McCalley, D. V. *Analyst* **1990**, *115*, 1355–1358.

spatially accessible for successful recognition by the hydroxyl group of methyl paraben (cf. Figure 1a).

In view of this, we have first attempted to yield co-crystals from a mixture of methyl paraben, quinine, and quinidine in an equimolar ratio (1:1:1) in ethanol under slow evaporation. The resulting material was rather amorphous, so that it proved difficult not only to differentiate between pure quinine and quinidine, respectively, but also to identify possible co-crystal formation (i.e., due to broad, rather featureless signals in the respective ^{13}C CPMAS spectra). This prompted us to reconsider the co-crystallization technique (i.e., controlled cooling versus slow solution cooling of the respective materials). Therefore, we dissolved equimolar amounts of quinidine and methyl paraben in a solvent mixture of hexane and ethanol and left it for slow cooling in a thermostat. After 4 days, a white microcrystalline powder precipitated, which was identified as pharmaceutical co-crystal **1** of quinidine and methyl paraben (on the basis of its ^{13}C CPMAS NMR spectrum; cf. Figure 7a). However, when the experiment was similarly repeated with an equimolar mixture of quinine and methyl paraben, no precipitation occurred. Notably, we tried solvents such as acetone or toluene as well, but no precipitation occurred.

In another experiment, we dissolved an equimolar mixture of *quinidine*, *quinine*, and *methyl paraben* in a hexane−ethanol mixture. This time, after slow cooling for about 4 days, a white microcrystalline powder of quinidine−methyl paraben co-crystal **1** precipitated, leaving quinine in solution. Indeed, the white powder was identified on the basis of the ^{1}H and ^{13}C CP MAS NMR spectra (cf. Supporting Information), which were *almost identical* to the ^{1}H and ^{13}C CPMAS spectra of the co-crystal **1** (shown in Figures 3c and 7a, respectively). In addition, we repeated the experiment with an excess of methyl paraben (i.e., using a 2:1:1 ratio of methyl paraben, quinidine, and quinine), which again yielded quinidine−methyl paraben co-crystal **1** while quinine *and* excess methyl paraben remained in solution. Notably, the corresponding ^{13}C CPMAS spectrum of the rather amorphous mixture obtained from concentrating the remaining solution (in a rotary evaporator) revealed *no traces* of quinidine (^{13}C CPMAS spectra of pure quinidine, pure quinine, and the mixture of both with methyl paraben are given in the Supporting Information), thus confirming *complete* extraction of quinidine in the form of co-crystal **1** (cf. Figure 9).

Since crude extracts from naturally occurring *Cinchona* tree bark contain a rather large excess of quinine, as well as further alkaloids,[64] current work is in progress to reveal the full potential of co-crystallization as a means of separation.

3. Conclusion

In this work, we have successfully demonstrated the applicability of the O−H···N heterosynthon for the synthesis of a *pharmaceutical co-crystal* of the commonly used excipient methyl paraben and quinidine, an anti-malarial constituent of *Cinchona* tree bark. The co-crystal crystallizes in an orthorhombic space group, where the asymmetric unit is comprised of a hydrogen-bonded 1:1 complex of quinidine and methyl paraben. Complementary insights into local conformation and hydrogen-bonding were derived from multinuclear solid-state NMR and discussed with respect to NMR-based crystallography of structurally less-defined co-compounds, where an interpretation of the obtained NMR data was supported by DFT quantum-chemical computations. Furthermore, a means of selective separation of quinidine from its stereoisomer based on the *molecular specificity* of methyl paraben, which acted as "*molecular hook*" or "*single-armed*" *molecular tweezer* picking its target via hydrogen-bond-mediated molecular recognition, is presented.

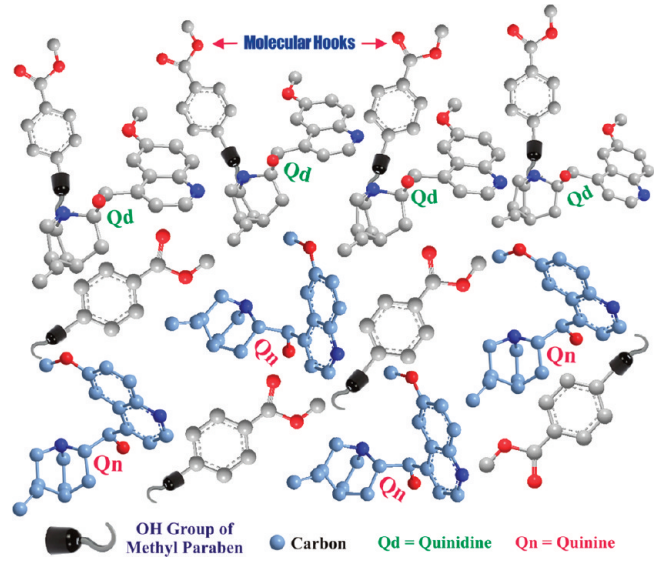

Figure 9. Schematic representation illustrating the use of methyl paraben as "*molecular hook*". The hydroxyl groups of the excipient methyl paraben selectively interact with quinidine molecules, thus allowing us to isolate them from a 1:1:2 mixture of quinidine, quinine, and methyl paraben. The excess of both methyl paraben and quinine remained in the solution.

4. Experimental Section

Quinidine ((9*S*)-6′-methoxycinchonan- 9-ol), quinine ((*R*)-(6-methoxyquinolin-4-yl)-((2*S*,4*S*,8*R*)-8-vinylquinuclidin-2-yl)methanol), and methyl paraben (methyl 4-hydroxybenzoate) were purchased from Aldrich and used as obtained. Co-crystals of methyl paraben and quinidine were prepared by dissolving 1 mmol of quinidine (324.4 mg) and 1 mmol of methyl paraben (152.15 mg) in 50 mL of ethanol (acetone can also be used) and left for slow evaporation in an open container. After 2 days, colorless prism-like crystals were obtained and subsequently ground to small microcrystalline particles for structurual characterization via powder diffraction (Supporting Information) and solid-state NMR. In order to obtain sufficiently large crystals suitable for single-crystal X-ray analysis, the same solution was left for slow evaporation in a test tube.

Quinidine Extraction. Co-crystallization of quinidine and quinine with methyl paraben in a 1:1:1 ratio was performed by stirring 0.5 mmol of quinidine (162.2 mg), 0.5 mmol of quinine (162.2 mg), and 0.5 mmol of methyl paraben (76.07 mg) in 25 mL of hexane at ∼80 °C, and then ethanol was added dropwise until a clear solution was obtained. The hot solution was then filtered (without allowing it to cool) and kept in the thermostat at 60 °C. After controlled cooling over a period of about 100 h from 60 to −10 °C, a white crystalline powder was obtained, which was filtered and characterized by ^{13}C CPMAS NMR and powder diffraction. Both types of spectra (Supporting Information) were found to be identical to the spectra of co-crystals of quinidine and methyl paraben, confirming successful isolation of quinidine co-crystal from the mixture. In addition, when the experiment was repeated with an excess of methyl paraben (i.e., 1:1:2 ratio: 162.2 mg of quinidine, 162.2 mg of quinine, and 152.1 mg of methyl paraben) similar results were found: that is, binary co-crystals of quinidine and

(64) Gatti, R.; Gioia, M. G.; Cavrini, V. *Anal. Chim. Acta* **2004**, *512*, 85–91.

methyl paraben precipitated as white microcrystalline powder, whereas residual quinine and excess methyl paraben remained in the solution.

Solid-State NMR Methods. Proton solid-state NMR data were recorded at 850.1 MHz employing a Bruker Avance III spectrometer, while additional ^{13}C CPMAS and ^{2}H MAS NMR spectra were recorded at 125.77 and 46.7 MHz, using Bruker Avance-II 300 and Bruker Avance 500 machines, respectively. Most experiments were carried out using a commercially available Bruker 1.3 mm double-resonance MAS probe at a spinning frequency of 50 kHz, typical $\pi/2$ pulse lengths of 2 μs, and recycle delays of 5−10 s. The spectra were referenced with respect to tetramethylsilane (TMS) using solid adamantane as secondary standard (1.63 ppm for ^{1}H and 29.456 ppm for ^{13}C); ^{2}H spectra were referenced with respect to solid dimethylsulfone (DMS, 3.4 ppm). In addition, ^{15}N CPMAS spectra were recorded at 30.4 MHz using a Bruker Avance-II 300 machine and referenced to solid $^{15}NH_4Cl$ (−341.0 ppm). If not stated otherwise, all spectra were collected at room temperature. The back-to-back (BaBa)[65] recoupling sequence was used to excite and reconvert double-quantum coherences, applying States-TPPI[66] for phase-sensitive detection. Further details are given in the figure captions of the respective 2D spectra.

DFT-Based Chemical Shift Calculations. Where necessary, proton positions of selected fragments (i.e., the asymmetric unit) of the investigated compounds were optimized (with all heavy atoms fixed at the crystallographic positions) by DFT-based quantum chemical calculations using the B3LYP functional and 6-311G[67] split valence basis set augmented with diffuse and polarization functions. Subsequently, ^{1}H, ^{13}C, and ^{15}N chemical shifts with respect to TMS (^{1}H), benzene and methanol (^{13}C), or nitromethane (^{15}N) were computed at the B3LYP/6-311+G** level of theory with the GIAO approach as implemented in the Gaussian03 program.[68] Note that the recently introduced multi-standard approach is applied in the case of ^{13}C.[56]

Single-Crystal Structure Analysis. Crystal parameters of **1** are reported as follows: colorless prism-like crystals with formula $C_{28}H_{32}N_2O_5$, orthorhombic $P2_12_12_1$ (No. 19) space group; $Z = 4$, $a = 9.962$ Å, $b = 11.497$ Å, $c = 22.710$ Å. Data collection at 120 K was done on a Nonius KCCD diffractometer (Mo Kα ($\lambda = 0.71073$ Å)), equipped with a graphite monochromator. Intensity data were corrected for Lorentz and polarization effects. Structure solution and refinement was performed employing the SHELXS86[69] and CRYSTALS[70] software packages. All non-hydrogen atoms were refined in the anisotropic approximation against F of all observed reflections. The hydrogen atoms were refined in the riding mode with fixed isotropic temperature factors; for **1**, R-factor (%) = 3.74. An independent determination of the absolute configuration was not attempted since pure quinidine was used in the crystallization experiments. In addition, Mo Kα radiation under the chosen experimental conditions is not favorable for determination of the absolute configuration.

Acknowledgment. Financial support from the Deutsche Forschungsgemeinschaft (DFG) through the SFB 625 in Mainz is gratefully acknowledged.

Note Added after ASAP Publication. References 9d and 11d were incorrect in the version of this article published ASAP March 17, 2010. The corrected references were published March 22, 2010.

Supporting Information Available: Spectral data not figured in the manuscript such as powder diffraction data and both ^{1}H and ^{13}C solution NMR spectra of pure quinidine, methyl paraben, and co-crystal **1**; a DSC stack plot for quinidine, methyl paraben, and co-crystal **1**; $^{1}H-^{1}H$ DQ spectra of pure quinidine and methyl paraben; solid-state ^{13}C CPMAS spectra of extracted co-crystal **1**, pure quinine, quinidine, and residual mixture as well as table of resonance assignments; CIF file of co-crystal **1**; and complete ref 68. This material is available free of charge via the Internet at http://pubs.acs.org.

JA100146F

(65) (a) Geen, J.; Titman, J.; Gottwald, J.; Spiess, H. W. *Chem. Phys. Lett.* **1994**, *227*, 79–86. (b) Gottwald, J.; Demco, D. E.; Graf, R.; Spiess, H. W. *Chem. Phys. Lett.* **1995**, *243*, 314–323. (c) Sommer, W.; Gottwald, J.; Demco, D. E.; Spiess, H. W. *J. Magn. Reson.* **1995**, *A 113*, 131–134. (d) Feike, M.; Demco, D. E.; Graf, R.; Gottwald, J.; Hafner, S.; Spiess, H. W. *J. Magn. Reson.* **1996**, *A122*, 214–221. (e) Saalwächter, K.; Graf, R.; Spiess, H. W. *J. Magn. Reson.* **1999**, *140*, 471–476. (f) Saalwächter, K.; Graf, R.; Spiess, H. W. *J. Magn. Reson.* **2001**, *148*, 398–418.

(66) Marion, D.; Ikura, M.; Tschudin, R.; Bax, A. *J. Magn. Reson.* **1989**, *85*, 393–399.

(67) Krishnan, R.; Binkley, J. S.; Seger, R.; Pople, J. A. *J. Chem. Phys.* **1980**, *72*, 650–654.

(68) Frisch, M. J.; et al. *Gaussian 03*, Revision D.02; Gaussian, Inc.: Wallingford, CT, 2004.

(69) Sheldrick, G. M. *SHELXS-86, Program package for crystal structure solution and refinement*; Univeristät Göttingen: Germany, 1986.

(70) Betteridge, P. W.; Carruthers, J. R.; Cooper, R. I.; Prout, K.; Watkin, D. J. *J. Appl. Crystallogr.* **2003**, *36*, 1487–1487.